

We are IntechOpen, the world's leading publisher of Open Access books Built by scientists, for scientists

5,000

Open access books available

125,000

International authors and editors

140M

Downloads

Our authors are among the

154

Countries delivered to

TOP 1%

most cited scientists

12.2%

Contributors from top 500 universities



WEB OF SCIENCE™

Selection of our books indexed in the Book Citation Index
in Web of Science™ Core Collection (BKCI)

Interested in publishing with us?
Contact book.department@intechopen.com

Numbers displayed above are based on latest data collected.

For more information visit www.intechopen.com



Characterization of Grafted Acrylamide onto Pine Magnetite Composite for the Removal of Methylene Blue from Wastewater

*Kgomotso N.G. Mtshatsheni, Bobby E. Naidoo
and Augustine E. Ofomaja*

Abstract

Much attention has been focused on chemical modification of natural biomass through grafting. Modification of natural polymers by graft copolymerization has shown to be a promising technique as it functionalizes a biopolymer to its potential, imparting desirable properties onto them. The present study focuses on functional groups such as $-\text{CO}-\text{NH}_2$ which were grafted into cellulose from acrylamides. The characterization of the composite was done using Fourier transform infrared spectroscopy (FTIR), X-ray diffraction (XRD), scanning electron microscopy (SEM), Brunauer-Emmett-Teller (BET), thermal gravimetric analysis (TGA), and transmission electron microscopy (TEM). These techniques were used to further demonstrate the formation of the grafted acrylamide composite (GACA). SEM analyses showed existence of strong chemical interactions between pine cone magnetite and acrylamides.

Keywords: characterization, adsorption, acrylamide, methylene blue, grafting

1. Introduction

The rapid development of the textile industry has resulted to a large proportion of industrial wastewater pollution. Methylene blue (MB) dye is a most widely used dye by industries like textile, paper, rubber, plastics, leather, cosmetics, food industries and pharmaceuticals. The textile industry is classified into three main categories, namely; cellulose fibers (cotton, rayon, linen, ramie, hemp and lyocell), protein fibers (wool, angora, mohair, cashmere and silk) and synthetic fibers (polyester, nylon, spandex, acetate, acrylic, ingeo and polypropylene) [1]. The type of dyes and chemicals used in the textile industry are found to differ depending on the fabrics manufactured. Reactive dyes (remazol, procion MX and cibacron F), direct dyes (congo red, direct yellow 50 and direct brown 116), naphthol dyes (fast yellow GC, fast scarlet R and fast blue B) and indigo dyes (indigo white, tyrian purple and indigo carmine) are some of the dyes used to dye cellulose fibers [1]. The textile industry is known to be the main creator of wastewater effluents because it

consumes more water for its wet processes. Therefore, globally it is estimated that all wastewater discharge is highly populated. According to the world bank estimation, textile dyeing and finishing treatment given to a fabric generates at least 17–20% of world's industrial wastewater [2, 3].

Dyes often discharged in water effluents contain residues that are highly visible and undesirable even at low concentrations [4]. In addition, they are toxic due to their harmful effects on the human beings. Therefore, it is of vital importance that they are removed from water [5]. Wastewater containing dyes needs to be treated before being discharged into water bodies [6]. Various techniques including chemical oxidation, coagulation-flocculation, membrane processes and biological treatment have shown effectiveness in the removal of methylene blue from waste water [7]. The limitation most of these techniques possess is the incomplete dye removal, poor detection, requirement of expensive equipment and monitoring systems [6]. The performance of adsorption techniques have been applied due to their effectiveness since they remove the entire dye molecule, leaving no fragments in the effluent [8].

Extensive research in recent years has focused on utilizing waste materials from agricultural products (such as pine cones and others) since they are eco-friendly, cost-effective and renewable [9]. Pine cones are naturally occurring agricultural wastes widely found in a plantation in Vanderbijlpark, Gauteng, South Africa. They are of commercial importance and value which is extensively used in different industries [10]. One pine cone consists of 46.5% hemicellulose, 37.4% lignin, 18.8% cellulose and 15.4% extractives [11]. Pine cone powder has been studied extensively in the removal of heavy metal pollutants such as lead, caesium, copper nickel and arsenic from water systems. Activated carbon has been the most employed adsorbent for the removal of dyes due to its outstanding adsorption properties. However, it has limitations by being expensive and it cannot be used in large applications of wastewater treatment. The use of biomass and other microbial cultures in the removal of methylene blue has been extensively studied in recent years. Among others, carbonized organic materials, fly ashes, peat moss, recycled alum sludge, fishery residues and microorganisms such as fungus and algae [12].

The present study reports the development and characterization of grafted pine magnetite composite using grafted acrylamide (GACA) for the removal of methylene blue in wastewater. Grafting is a process of chemically or physically manipulating the surface properties of plant materials such as type and amount of functional groups, surface area and porosity by extraction of plant chemical components in order to improve its adsorptive ability. Grafting of synthetic monomers onto pure biological materials has been successfully performed, e.g., grafting of acrylonitrile onto starch [13] and methyl acrylonitrile onto cotton [14].

2. Materials and methods

2.1 Materials

Pine cones are naturally occurring agricultural wastes found in a plantation in Vanderbijlpark, Gauteng, South Africa. All the chemicals and reagents used throughout this study were of analytical grade reagents and used without any further purification. Acrylicamide, ceric ammonium nitrate (CAN), nitric acid (HNO_3), sodium hydroxide (NaOH), ammonium hydroxide (NH_4OH), ferric sulfate (FeSO_4) and methylene blue was supplied by Merck, South Africa. Deionized water was used for the preparation of all solutions. The stock solution for methylene blue (1000 mg/L) was prepared by dissolving the required amount of dyes in a 1000 ml of deionized water and the stock solution was further diluted for batch experiments.

2.2 Methods

2.2.1 Synthesis of pine-magnetite composites

A mixture of $\text{FeSO}_4 \cdot 7\text{H}_2\text{O}$ (2.1 g) and of $\text{Fe}(\text{SO}_4)_3 \cdot \text{XH}_2\text{O}$ (3.1 g) were dissolved under inert atmosphere in 100 cm^3 of double-distilled water with vigorous stirring. Thereafter, 20 cm^3 of 28% ammonium hydroxide and the appropriate amount of pine powder was added. The reaction was left to run for 45 min at 80°C under constant stirring. The resulting particles, consisting of magnetite attached to the cellulose (hereafter referred to as bio-composite) were washed several times with deionized water and ethanol and dried in a vacuum oven at 60°C overnight. To determine the optimum conditions to achieve the desired products of the biocomposites, we experimented with the following variables: volume of NH_4OH 5, 10, 20, 30, and 40 cm^3 ; weight of pine powder 1.0, 1.5, 2.0, 2.5, 3.0 and 3.5 g; temperatures 40, 60, 80 and 100°C and reaction times 15, 30, 45 and 60 min.

2.2.2 Synthesis of grafted pine magnetite composite

1 g of pine magnetite composite (PMC), 20 ml of 1.5 M acrylamide and 135 ml of deionised water were transferred into a three neck round bottom flask at a temperature of 42°C . The reaction was bubbled under nitrogen gas for 30 min to remove the dissolved oxygen under stirring. 10 ml of 0.5 M CAN, dissolved in 0.3 M HNO_3 was slowly added to the reaction to initiate graft co-polymerization and stirring was continued for 2 h. Reaction mass was neutralised by 50% NaOH and precipitated in methanol and thereafter washed with methanol/water (90:10) several times, so that the unreacted PMC and ceric salt were removed. The final residue was dried in a vacuum oven at 40°C .

2.3 Characterization

Qualitative and fundamental identification of the functional chemical groups of grafted pine magnetite composite (GPMC) were carried out with a FTIR (Perkin-Elmer) in the range $450\text{--}4000 \text{ cm}^{-1}$. An X'Pert PRO X-ray diffractometer (PAN analytical, PW3040/60 XRD; $\text{CuK}\alpha$ anode; $\lambda = 0.154 \text{ nm}$) was used for particle size measurements. The size of the synthesized particles was observed using transmission electron microscope (TEM, FEI TECNAI G² SPIRIT) at an accelerating voltage of 150 kV. TGA (Perkin-Elmer (USA) Simultaneous Thermal Analyzer 6000 instrument) was used for determining the weight loss as a function of temperature. Changes in morphology were studied using scanning electron microscopy (SEM), HRSEM Instrument Specs Model: Jeol JSM 7800F field emission scanning electron microscope run operational voltage: 5kVEDS specs Model: Thermo Fischer UltraDry EDS Detector for the graft co-polymerization and incorporation of iron oxide magnetite (Fe_3O_4 PMC).

3. Results and discussions

3.1 FT-IR spectroscopy results

The FT-IR spectrum shown in **Figure 1(a)** represents the pine- Fe_3O_4 magnetite (PMC). The FT-IR spectrum showed some changes in band intensities, indicating the functional groups on the surface that had been modified. A compressed —OH peak at 3350 cm^{-1} with an increase in intensity was observed. This might have been

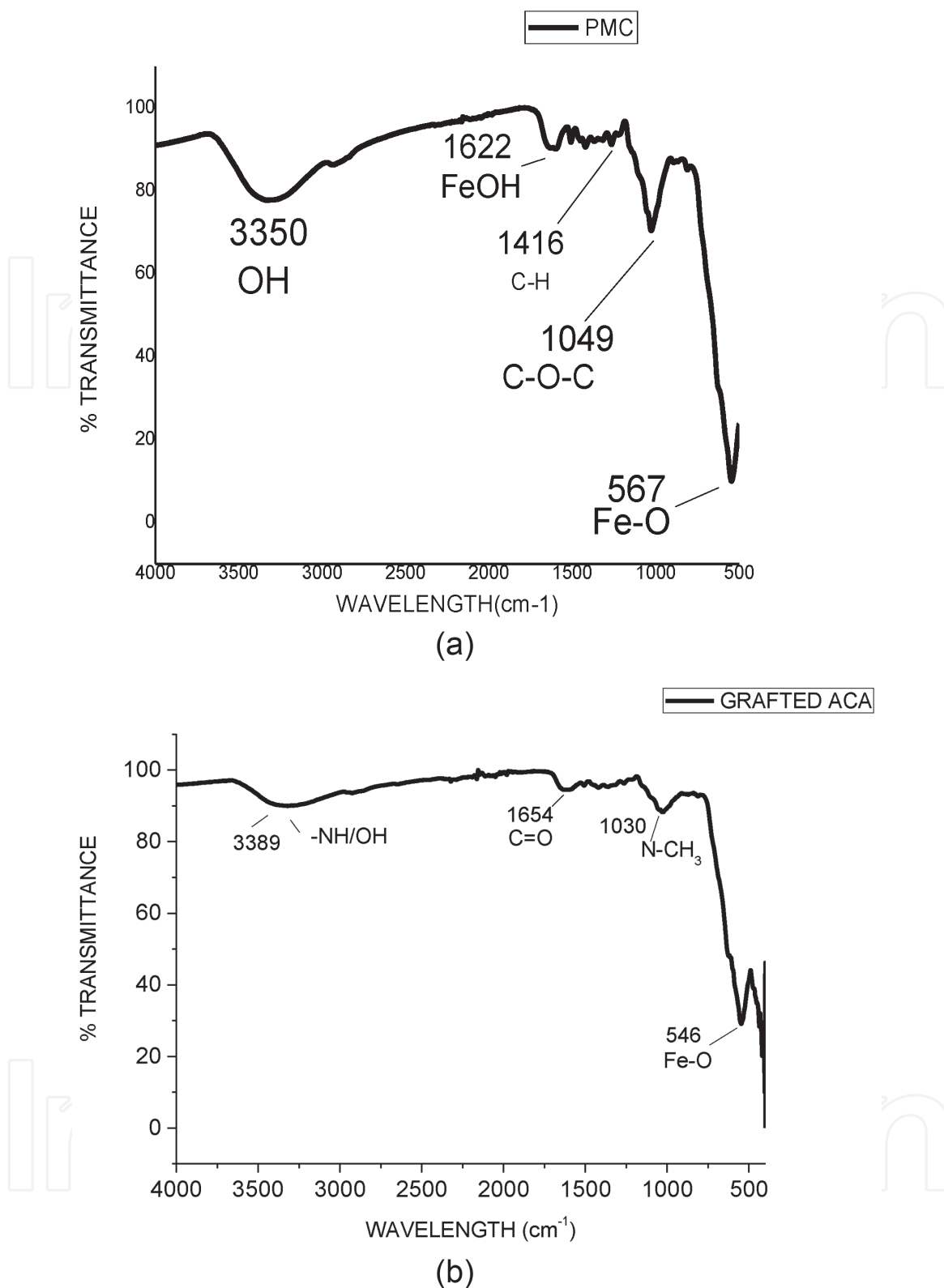


Figure 1.
(a) FT-IR spectrum for PMC and (b) FT-IR spectrum for GACA.

due to the presence of extracted lignin in pine cone. Clearly, the COO— peak was converted to esters at 1622 cm⁻¹, C—H aliphatic peaks were observed at 1416 cm⁻¹ which represent the increase in the internal surface of the pine cone and a new peak was found at 567 cm⁻¹ which was assigned to the vibration of Fe—O band of Fe₃O₄.

The FT-IR spectrum of GACA (**Figure 1(b)**) shows a slightly broad band observed at 3389 cm⁻¹ ascribed to the existence of OH— and —NH groups [15]. The compressed peak at 1654 cm⁻¹ corresponds to a carbonyl functional group of

acrylamide [16, 17], whereas the one at 1030 cm^{-1} reflects on the vibrations of N—CH₂ groups. The last peak at 546 cm^{-1} reflects the Fe—O functional groups. These functional groups might have participated in the interactions with MB which involved the mechanism of surface complex, hydrogen bonding, and electrostatic attractions.

3.2 XRD analyses

The XRD spectrum of grafted pine magnetite composite with acrylamide is shown in **Figure 2a**. The prominent peaks at 2θ values of 30.5° , 38.7° , 43.9° , 59.8° and 63.7° corresponding to (220), (311), (400), (422), (511), respectively, attributes to the cellulose peaks due to the presence of iron oxide magnetite composite and crystal planes of grafted pine magnetic composite respectively [18]. The composite has shown a cubic crystal structure. It is observed that diffraction intensity of the broad peak at 43.9° was weakened indicating that the crystallinity of the PMC decreased after grafting. This phenomenon might be due to the strong interaction of covalent bonds between the PMC and the acrylamide.

3.3 TGA analyses

The TGA and DTG curves shown in **Figure 3a** demonstrate the thermal stability of grafted pine magnetite composite. The incorporation of the Fe₃O₄ magnetite composite showed the changes in the thermal properties of the cellulose. The initial thermal decomposition of GACA occurred at $100\text{--}240^\circ\text{C}$ temperature range which corresponds to loss of water molecules and volatile compounds. The second stage thermal decomposition in the temperature range $380\text{--}640^\circ\text{C}$ may be due to the breakdown of the polymer matrix and cross-links between different polymeric chains. The last stage of decomposition at a temperature of 700°C corresponds to the lignin degradation [19]. Grafting with acrylamide presented a better thermal stability due to the different types of covalent bonds in the grafting of copolymer backbone [20]. Differential thermal analysis (DTA) showed endothermic peaks associated with degradation of various materials. The degradation behaviour exhibited two stage decomposition effects. Observation at different temperatures ($380\text{--}620^\circ\text{C}$) was attributed to the cellulose decomposition at low temperature and grafted acrylamide composite at higher temperatures. This confirmed the stabilizing effect of the incorporation of Fe₃O₄ composite onto acrylamide.

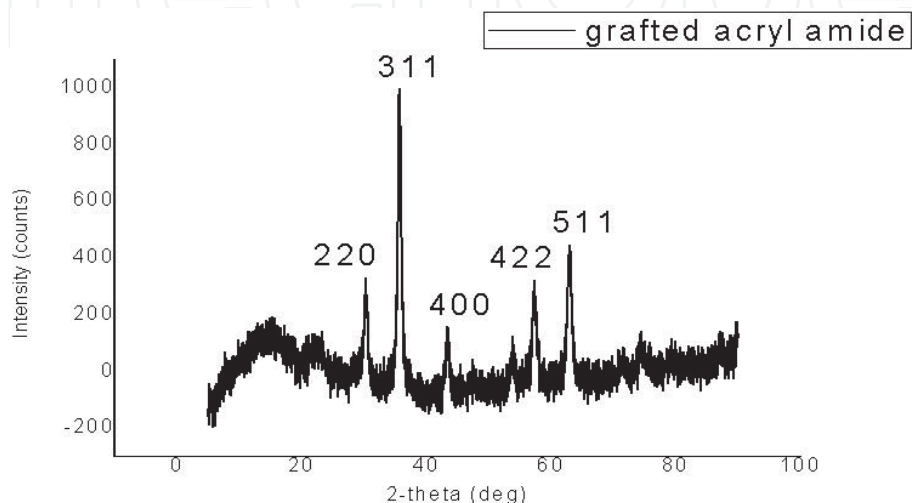


Figure 2.
XRD spectrum for GACA.

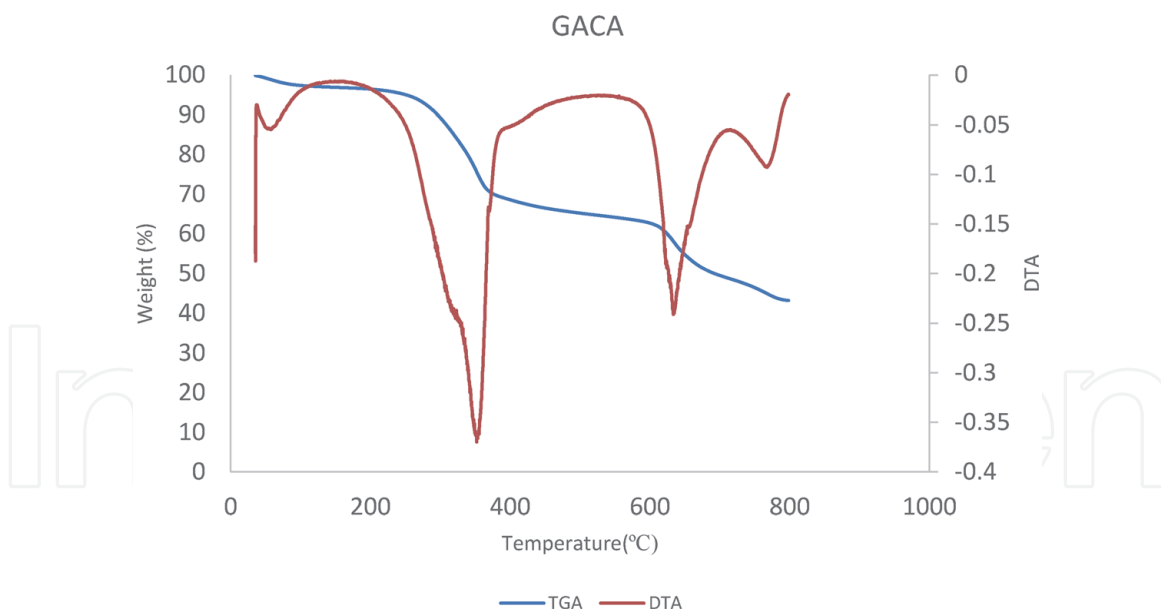


Figure 3.
TGA and DTA curves for GACA.

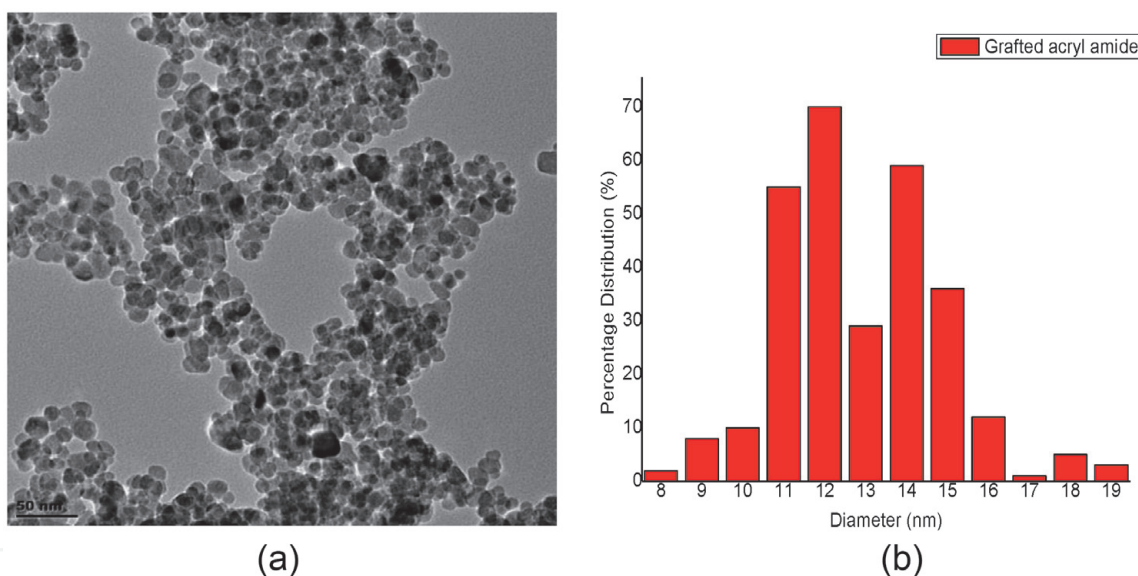


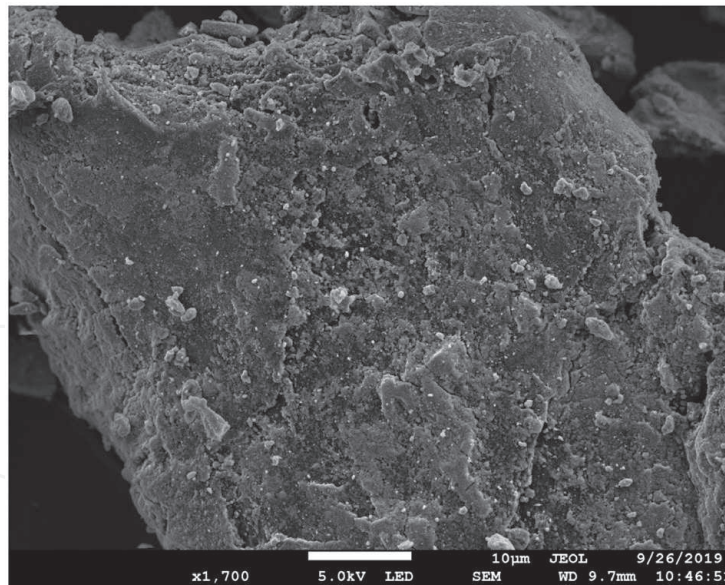
Figure 4.
(a) TEM image and (b) size distribution of GACA.

3.4 TEM studies

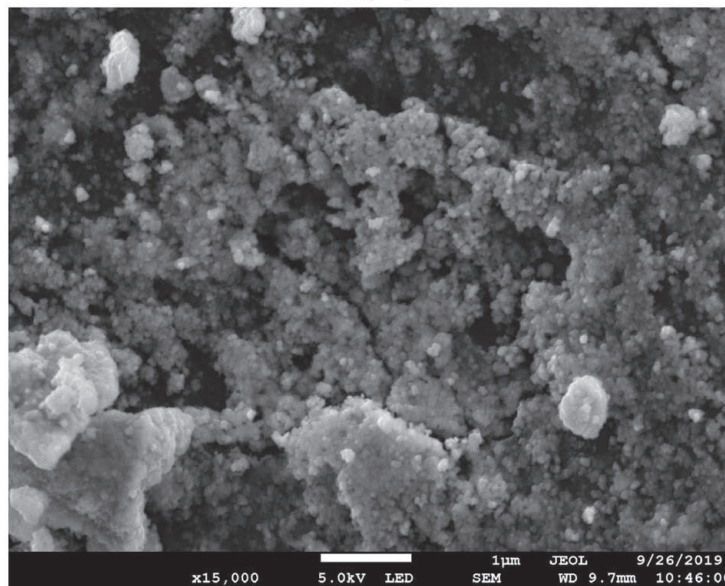
The TEM image in **Figure 4(a)** shows the appearance of the typical images of grafted pine magnetic composite with acrylamide. The supporting information showed spherical nano-particles as attributed to the shape and the incorporation of the magnetic nanoparticles in the polymer matrix. **Figure 4(b)** shows the size distribution of the pine magnetite particles with a peak at 12 nm.

3.5 SEM studies

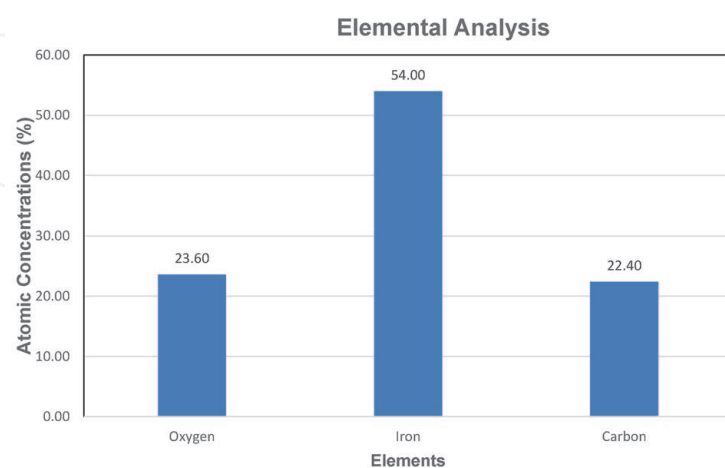
SEM images of grafted pine magnetite composite with acrylamide are shown in **Figure 5(a)** and **(b)**. The observation showed changes in morphology of the GACA



(a)



(b)



(c)

Figure 5. (a) SEM image of the GACA, (b) SEM image of the GACA and (c) elemental analysis from SEM-EDX.

because of the graft copolymerization process and incorporation iron oxide magnetite. Supporting information showed the granular smooth surface. Roughness of the surface increased after modification, better matrix coherence was achieved after incorporation of the iron oxide magnetite nanoparticles. All the observations confirmed that grafting pine magnetite composite with acrylamide allows better compatibility. The presence of the Fe peak in the EDX of the nanocomposite showed successful incorporation of iron oxide composite in the polymer matrix **Figure 5(c)**.

3.6 BET (surface area) analyses

A surface property of an adsorbent describes the effect of modification on the surface area of the adsorbent. **Table 1** shows comparison of the effect of modification on the surface area of the materials. The pure pine magnetite nanoparticles showed a surface area of 113.60 m²/g, pore volume of 0.6321 cm³/g and pore size of 25.86 nm. On the other hand, the NaOH treated pine had a surface area of 2.25 m²/g, pore volume of 0.0177 cm³/g and pore size of 10.17 nm. Pine magnetite composite exhibited surface area of 54.80 m²/g, pore volume of 0.1522 cm³/g and pore size of 23.10 nm. Grafted acrylamide reflected the surface area of 57.77 m²/g, pore volume of 0.1591 cm³/g and pore size of 17.33 nm. The higher surface area was due to the pine cone structure which was found to be important for the improvement of mass diffusion and adsorptive capacity. An increase in surface area, pore volume and pore size confirmed that GACA can adsorb MB more efficiently than the PMC. The distinct pore structure size enables fast transportation of particles.

3.7 Point zero charge (pH_{pzc})

To further investigate the effects of modifications on the suitability of the synthesized materials for adsorption, the isoelectric point or point of zero charge (pH_{pzc}) was determined. The solution pH is an important parameter for dye adsorption because it does not only change the surface charge of the adsorbent but also it affects the molecular structure of the dye. As MB is a cationic dye, it can easily form positively charged species over a wide pH range. The solid addition method was used to determine the pH_{pzc} of the pine cone composite. To a series of 100 cm³ volumetric flasks, 45 cm³ of 0.01 mol/dm³ KNO₃ solution were transferred. The pH_i values of the solutions were roughly adjusted between pH 2 and 12 by the addition of either 0.1 mol/dm³ HCl or NaOH on a pH meter with constant stirring. The total volume of the solution in each flask was made up to 50 cm³ by the addition of KNO₃ solution of the same strength. The pH_i of the solutions was accurately noted, and 0.1 g of pine cone composite were added to each volumetric flask, which was then immediately closed. The suspensions were allowed to equilibrate for 48 h on a shaker operating at 200 rpm. The pH_f values of the supernatant were accurately noted and the difference between the initial and final pH values ($\Delta\text{pH} = \text{pH}_f - \text{pH}_i$) were plotted against the pH_i. The solution pH is an important parameter for

Properties	Pure magnetite composite	NaOH treated pine	Pine magnetite composite (PMC)	Grafted acrylamide
Surface area (m ² /g)	113.60	2.25	54.80	57.77
Pore volume (cm ³ /g)	0.6321	0.0177	0.1522	0.1591
Ave. pore size (nm)	25.86	10.17	23.10	17.33

Table 1.
BET surface area and pore characteristics for synthesized materials.

dye adsorption because it does not only change the surface charge of an adsorbent, but it also reflects the molecular structure of the dye.

Changes in the point of zero charge values within the sample can be attributed by the difference in types and amounts of surface functional groups present on the surface of the adsorbent. pH_{pzc} is observed when modification on the suitability of the synthesized materials is determined. It is known to be the pH at which the amount of positive charges on a biosorbent surface equals the amount of the negative charge, i.e., the pH at which the biosorbent surface has net electrical neutrality [21, 22]. Methylene blue is a cationic dye and can easily form positively charged species over a wide pH range. The pH_{pzc} of pine magnetite composite was found to be 8.56 and grafted pine magnetite with acrylamide was found to be 6.2. The decrease in the pH_{pzc} is attributed to the modification of the surface area.

3.8 Adsorption studies

3.8.1 Effect of solution pH

The adsorption experiments were carried out using batch equilibration techniques. Various methylene blue (MB) solutions with different pH range, initial concentrations and mass dosage were prepared by diluting 1000 mg/dm^3 . Equilibrium experiments, to determine the adsorption capacity of pine magnetite composite were conducted using 250 cm^3 bottles. 0.1 g of PMC and 100 cm^3 of the MB solution were added and shaken for 2 h at 26°C . Thereafter, absorbance was determined using UV-VIS spectrophotometer at the wavelength corresponding to the maximum absorbance ($\lambda_{\text{max}} = 665 \text{ nm}$) as determined from the plot. This wavelength was used for measuring the absorbance of residual concentration of MB. pH of the solution was adjusted using 0.1 M HCl and 0.1 M NaOH . **Figure 6** showed the effect of pH on the adsorption of MB. An increase in pH showed an increase in percentage removal. When the pH was 2.0 and 4.0, the removal rate of MB was 99.4 and 99.5%, respectively. This indicated that the lower adsorption of MB at acidic pH was due to the presence of excess H^+ ions. The influence of low pH to MB adsorption was that H^+ ions could occupy the binding sites; this was not favorable for the adsorption of MB. Furthermore, MB possessed positive surface charges and could be repulsed by H^+ ions to prevent MB adsorption onto grafted pine magnetic composite.

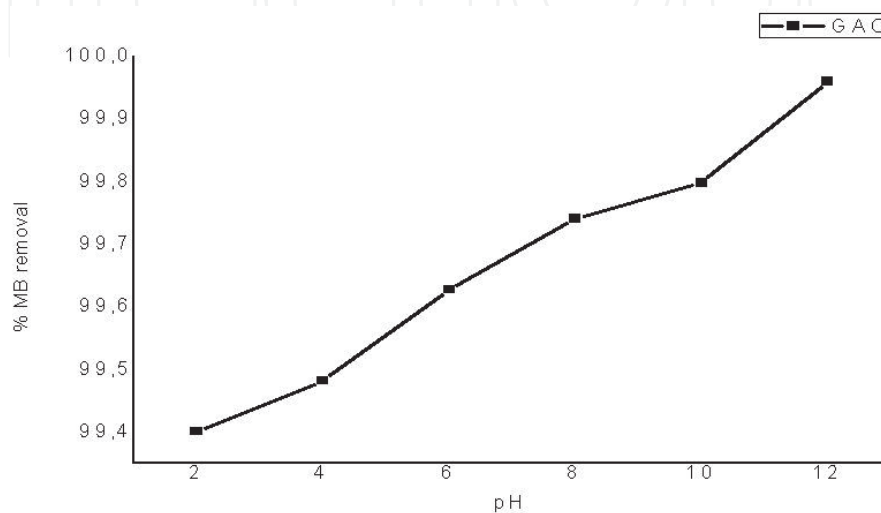


Figure 6.
Effect of pH on the adsorption of MB.

With increasing pH, the number of hydrogen ions in solution was reduced and the competitive effect, repulsive interaction weakened, lead to an increase in the removal rate. The MB removal rate became stable when the pH reached 12, where the higher percentage removal for MB was observed in comparison to other pH values.

3.8.2 Effect of adsorbent dose

Figure 7 shows the effect of adsorbent dose on the percentage removal and amount of dye that was adsorbed. This effect was necessary in order to observe how the novel adsorbent used impacted on the adsorption stoichiometry. It also gave an idea of the propensity of dye molecules to be adsorbed with the smallest amount of adsorbent. When the mass of the adsorbent was 0.5 g, the percentage adsorption removal increased rapidly, which contributed to the increased surface area of the adsorbent which in turn increased the number of binding sites [23]. The adsorption capacity decreased as the amount of adsorbent GACA increased because more active sites were available for the adsorption of dye, which resulted in more interactions between dye and adsorbent thus increasing the MB percentage removal. At mass 0.5 g the highest percentage removal of 99.8% was achieved.

3.8.3 Effect of contact time

The effect of contact time on the grafted pine magnetite composite with acrylamide for the adsorption of methylene blue is shown in **Figure 8**. The adsorption experiment was done at 100 mg/L concentration. The adsorption rate of the grafted composite on the removal of MB is faster from the beginning which might be influenced by the grafted composite with higher specific gravity which makes them better in dispersity and more efficient contact with MB. The adsorption capacity of the grafted composite is higher due to its high surface area.

3.9 Adsorption isotherms

The adsorption isotherm explains the relationship between an adsorbate in the liquid phase and the adsorbate adsorbed on the surface of the adsorbent at

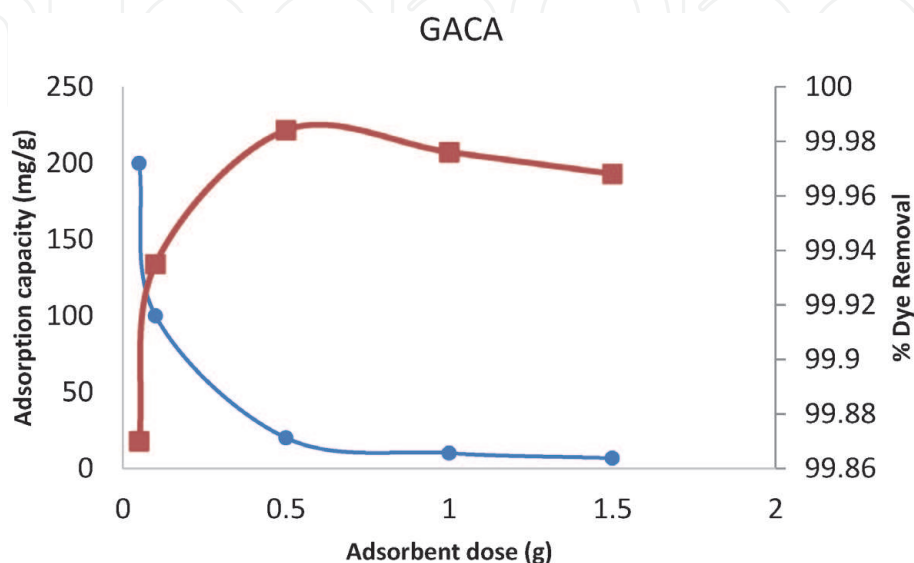


Figure 7.
Effect of adsorbent dose on the adsorption of MB.

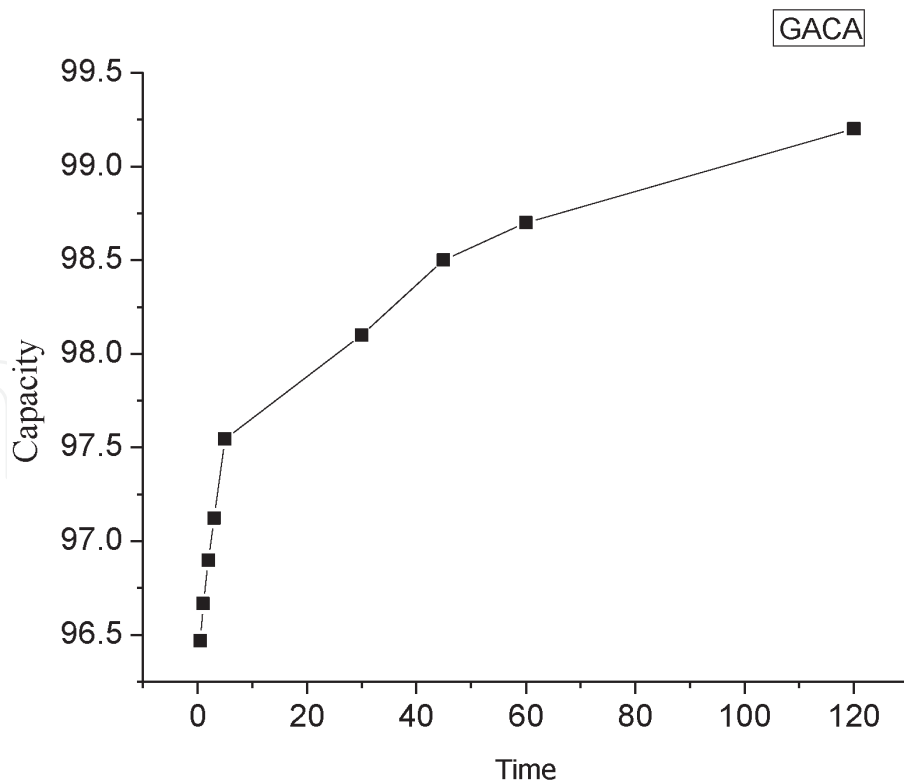


Figure 8.
 Effect of contact time at 100 mg/L on the MB adsorption of the GACA.

equilibrium at constant temperature [24, 25]. To successfully obtain the adsorptive behaviour of any substance from the liquid to the solid phase, it is important to have a satisfactory description of the equilibrium state between two phases composing the adsorption system. Langmuir and Freundlich isotherms are the well-known isotherms which have been used to describe the equilibrium of adsorption systems. Typically, the Langmuir model describes the monolayer sorption on a surface containing a limited number of sites and predicting a homogeneous distribution of sorption energies [25]. Freundlich describe the heterogeneity distribution. The results of the MB concentration dependence study were subjected to analyses by using Langmuir and Freundlich isotherm models.

The theoretical Langmuir isotherm is represented by the following equation:

$$C_e/q_e = 1/q_m K_L + C_e/q_m \quad (1)$$

where q_e is the amount of dye adsorbed at the equilibrium time (mg/g), C_e is the equilibrium dye concentration (dm³/mg), q_m is the maximum adsorption capacity (mg/g) and K_L is the Langmuir adsorption equilibrium constant (dm³/mg). Freundlich linear expression was represented by:

$$\text{Log } q_e = \text{log } K_F + 1/n \text{ log } C_e \quad (2)$$

where K_F is the equilibrium adsorption coefficient (dm³/mg) and $1/n$ is an empirical constant. The parameters of the isotherm models are calculated from the experimental data and the values of correlation coefficient (R^2) are demonstrated in **Table 2**. The results show R^2 values for the Langmuir are higher than those of Freundlich isotherm model. This implies that the equilibrium adsorption data comply with the Langmuir isotherm, suggesting that the adsorption process occurs in a homogeneous surface. Also, it can be stated that the results demonstrate no interaction and transmigration of dyes in the plane of the neighboring surface [26].

Langmuir isotherm model				Freundlich isotherm model		
Temperature (K)	Q_m (mg/m)	K_L (dm ³ /mg)	R^2	K_f (mg/g) (dm ³ /mg)	N	R^2
299	57.47	0.2107	0.9957	17.7174	2.862	0.9819
304	82.64	0.0588	0.9745	7.66655	1.725	0.9635
309	78.74	0.0968	0.9825	10.7226	1.873	0.9691
314	68.03	0.1786	0.9851	15.01067	2.293	0.9097
319	67.11	0.2569	0.9925	18.02603	2.455	0.8879

Table 2.
Isotherm parameters for methylene blue dye adsorption on GACA.

Higher K_f value for GACA indicates a higher adsorption capacity for methylene blue and a value of $n > 1$ indicates favorable adsorption conditions [27, 28].

3.10 Desorption and regeneration

The main goal of desorption studies is the competitiveness of adsorbents reusability in the multiple adsorption or desorption cycles and their beneficial potential in practical and economical applications. Desorption studies were performed with 0.01 M, 0.05 M and 0.1 M HCl. Typically, 1 g of PMC saturated with 100 mg/L of MB was placed in different desorption solutions and constantly stirred in a water bath at 200 rpm for 2 h. The adsorbent solutions were centrifuged and analysed using UV-VIS spectrophotometer. **Figure 9(a)** demonstrates the effect of eluent concentrations on MB dye desorption efficiency. It was observed that desorption efficiency increased with increase in the eluent concentration even though the shift is small in percentage. The maximum desorption percentage was found at 0.1 M HCl (99.8%) whereby 0.01 M HCl showed the minimum desorption efficiency (98.8%). An increase in HCl concentration resulted in an increase in H⁺ ions concentration which led to a subsequent increase in dye desorption efficiency.

Regeneration shows the competitiveness of the adsorbent where it expresses the good reusability and recycling abilities. **Figure 9(b)** demonstrates the possibility of regeneration and reusability of the grafted pine magnetite composite with acrylamide. Adsorption-desorption reaction cycles were repeated 4 times using 0.1 M HCl

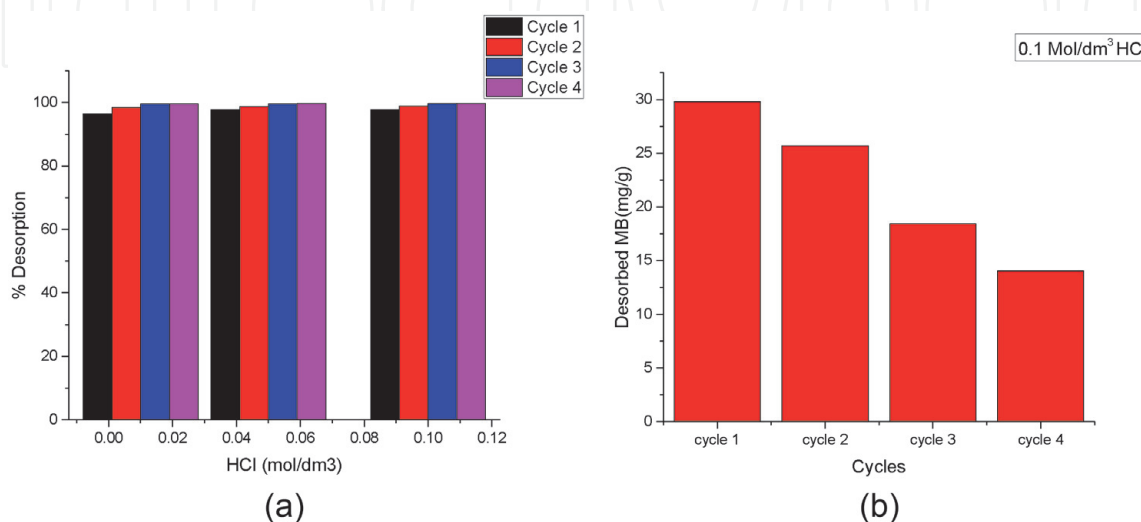


Figure 9.
(a) Desorption characteristics of MB adsorbed and (b) regeneration characteristics of MB adsorbed.

as the desorbing agent. Observation showed that there was a gradual reduction from 29.8% to 14.03% after cycle 4. The results explain that the higher adsorption capacity proves the adsorbent to be a good adsorbent for the removal of MB.

3.11 Conclusions

The study showed that acrylamide was successfully grafted onto pine magnetite composites. FT-IR, BET, SEM, TEM and XRD characterization provided sufficient evidence to demonstrate the incorporation and distribution of the iron oxide nanoparticles within the polymer matrix. GACA nanocomposites were shown to be effective in the adsorption of methylene blue at a pH of 12. The role of adsorbent dose and contact time demonstrated excellent results in the adsorption of methylene blue due to the increased surface area and high rate of the adsorption were achieved. The adsorption data was adequately interpreted by Langmuir and Freundlich isotherm models respectively. It was found that Langmuir isotherm model gave the best equilibrium fit.

Acknowledgements

We are grateful to Prof E.N. Nxumalo and Mr S.A. Zikalala for their contributions on the study. Vaal University of Technology and National Research Foundation of South Africa are thanked for financial support.


IntechOpen

Author details

Kgomotso N.G. Mtshatsheni*, Bobby E. Naidoo and Augustine E. Ofomaja
Department of Chemistry, Vaal University of Technology, Vanderbijlpark,
South Africa

*Address all correspondence to: kgomotsom@vut.ac.za

IntechOpen

© 2020 The Author(s). Licensee IntechOpen. This chapter is distributed under the terms of the Creative Commons Attribution License (<http://creativecommons.org/licenses/by/3.0>), which permits unrestricted use, distribution, and reproduction in any medium, provided the original work is properly cited. 

References

- [1] Ghaly AE, Ananthashankar R, Alhattab M, Ramakrishnan VV. Production, characterization and treatment of textile effluents: A critical review. *Journal of Chemical Engineering & Process Technology*. 2014;**5**:1
- [2] Holkar CR, Jadhav AJ, Pinjari DV, Mahamuni NM, Pandit AB. A critical review on textile wastewater treatments: Possible approaches. *Journal of Environmental Management*. 2016; **182**:351-366
- [3] Yaseen DA, Scholz M. Textile dye wastewater characteristics and constituents of synthetic effluents: A critical review. *International Journal of Environmental Science and Technology*. 2019;**16**:1193-1226
- [4] Amaral FM, Kato MT, Florêncio L, Gavazza S. Color, organic matter and sulfate removal from textile effluents by anaerobic and aerobic processes. *Bioresource Technology*. 2014;**163**: 364-369
- [5] Kausar A, Iqbal M, Javeda A, Aftab K, Nazli ZH, Bhatti HN, et al. Adsorption using clay and modified clay: A review. *Journal of Molecular Liquids*. 2018;**256**:395-407
- [6] Gbemeloluwa O, James H, Dong H. Biosorption of azure dye with sunflower seed Hull: Estimation of equilibrium, thermodynamic and kinetic parameters. *International Journal of Engineering Research and Development*. 2014;**10**(6): 26-41
- [7] Debnath S, Ballav N, Maity A, Pillay K. Competitive adsorption of ternary dye mixture using pine cone powder modified with β -cyclodextrin. *Journal of Molecular Liquids*. 2017;**225**:679-688
- [8] Sara D, Tushar KS. Review on dye removal from its aqueous solution into alternative cost effective and non-conventional adsorbents. *Journal of Chemical and Process Engineering*. 2014;**1**:104
- [9] Alshabanat M, Alsenani G, Almufarij R. Research article removal of crystal violet dye from aqueous solutions onto date palm fibre. *Chemistry*. 2013;**9**:1-6
- [10] Martin-Lara MA, Blazquez G, Calero M, Almendros AI, Ronda A. Binary biosorption of copper and lead onto pine cone shell in batch reactors and in fixed bed columns. *International Journal of Mineral Processing*. 2016;**148**: 72-82
- [11] Ofomaja AE, Naidoo EB, Modise SJ. Biosorption of copper (II) onto potassium hydroxide treated pine cone powder. *Journal of Environmental Management*. 2010;**91**(8):1674-1685
- [12] Lima EC, Royer B, Vagheti JPC, Simon NM, da Cunha BM, Pavan FA, et al. Application of Brazilian pine-fruit shell as a biosorbent to removal of reactive red 194 textile dye from aqueous solution. Kinetics and equilibrium study. *Journal of Hazardous Materials*. 2008;**155**(2008):536-550
- [13] Gao JP, Tian RC, Yu JG, Duan ML. Graft copolymers of methyl methacrylate onto canna starch using manganic pyrophosphate as an initiator. *Journal of Applied Polymer Science*. 1994;**53**:1091
- [14] Salam MA. Achieving competitive advantage through managing supply chain excellence: The case of Thai garment industry. *Journal of Textile and Apparel, Technology and Management*. 2005;**4**:1
- [15] Reena S, Rajiv ST, Nagpal AK. Effect of cross-linker and initiator concentration on the swelling behaviour and network parameters of superabsorbent hydrogels based on acrylamide and acrylic acid.

International Journal of Plastics
Technology. 2009;**13**:22-37

[16] Mohammad S, Behrouz H. Crosslinked graft copolymer of methacrylic acid and gelatin as a novel hydrogel with pH responsiveness properties. *Materials*. 2011;**4**:543-552

[17] Bhattacharyya R, Ray SK. Enhanced adsorption of synthetic dyes from aqueous solution by a semi interpenetrating network hydrogel based on starch. *Journal of Industrial and Engineering Chemistry*. 2014;**20**: 3714-3725

[18] Xu Z, Shen C, Tian Y, Shi XZ, Gao HJ. Organic phase synthesis of monodisperse iron oxide nanocrystals using iron chloride as precursor. *Nanoscale*. 2010;**2**:1027-1032

[19] Ofomaja AE, Ngema SL, Naidoo EB. Grafting of acrylic acid onto biosorbents: Effect of plant components and initiator concentration. *Carbohydrate Polymers*. 2012;**90**: 201-209

[20] Princi E, Vicini S, Pedemonte E, Mulas A, Franceschi E, Luciano G. Thermal analysis and characterization of cellulose modified with acrylic acid monomers. *Thermochimica Acta*. 2005; **425**:173-179

[21] Deng Y, Guo Y, Watson H, Au WC, Shakoury-Elizeh M, Basrai MA, et al. Gga2 mediates sequential ubiquitin-independent and ubiquitin-dependent steps in the trafficking of ARN1 from the trans-Golgi network to the vacuole. *The Journal of Biological Chemistry*. 2009;**284**(35):23830-23841

[22] Ofomaja AE, Naidoo EB, Modise SJ. Removal of copper(II) from aqueous solution by pine and base modified pine cone powder as biosorbent. *Journal of Hazardous Materials*. 2009;**168**:909-917

[23] Bhumik M, Leswif TY, Maity A, Srinivasu VV, Onyango MS. Removal of

fluoride from aqueous solution by polypyrrole/Fe₃O₄ magnetic nanoparticles. *Journal of Hazardous Materials*. 2011;**186**:150-159

[24] Li K, Wang X. Adsorptive removal of Pb(II) by activated carbon prepared from *Spartina alterniflora*: Equilibrium, kinetics and thermodynamics. *Bioresource Technology*. 2009;**100**(11): 2810-2815

[25] Shaibu SE, Adekola FA, Adegoke HI, Ayanda OS. A comparative study of the adsorption of methylene blue onto synthesized nanoscale zero-valent iron-bamboo and manganese-bamboo composites. *Materials*. 2014;**7**: 4493-4507

[26] Foo K, Hameed B. Preparation of oil palm (*Elaeis*) empty fruit bunch activated carbon by microwave assisted KOH activation for the adsorption of methylene blue. *Desalination*. 2011;**275**: 302-305

[27] Hameed BH, Mahmoud DK, Ahmad AL. Equilibrium modeling and kinetic studies on the adsorption of basic dye by a low-cost adsorbent: Coconut (*Cocos nucifera*) bunch waste. *Journal of Hazardous Materials*. 2008;**158**:65-72

[28] Hameed BH. Grass waste: A novel sorbent for the removal of basic dye from aqueous solution. *Journal of Hazardous Materials*. 2009;**166**:233-238